Pergamon

Polyhedron Vol. 16, No. 20, pp. 3641–3648, 1997
© 1997 Elsevier Science Ltd
All rights reserved. Printed in Great Britain
0277–5387/97 $17.00+0.00

PII: S0277-5387(97)00098-3

Syntheses and electrochemistry of metal complexes of a bulky pyridine–thiolate ligand

Wa-Hung Leung,[a]* Tom S. M. Hun,[a] Sherman Fung,[a] Ian D. Williams[a] and Kwok-Yin Wong[b]

[a] Department of Chemistry, The Hong Kong University of Science and Technology, Clear Water Bay, Kowloon, Hong Kong

[b] Department of Applied Biology and Chemical Technology, The Hong Kong Polytechnic University, Hunghom, Hong Kong

(Received 13 January 1997; accepted 28 February 1997)

Abstract—Reactions of Li(*t*BuL–NS) (lithium bis(4-*t*-butylphenyl)-2-pyridylmethanthiolate(1−)) with MCl_2 (M = Ni, Zn, Pt) afforded the respective $M(tBuL\text{–}NS)_2$ complexes in good yields. Treatment of $CuCl_2$, $Cu(OTf)_2$ (OTf = triflate) and $PdCl_2(PhCN)_2$ with Li(*t*BuL–NS) led to the formation of the dimeric compounds $[Cu(tBuL\text{–}NS)Cl]_2 \cdot 2H_2O$, $Cu_2(tBuL\text{–}NS)_3(OTf)$ and $[Pd(tBuL\text{–}NS)Cl]_2$, respectively. The interaction of Li(*t*-BuL–NS) with $[Ru(CO)_2Cl_2]_n$, $[Rh(COD)Cl]_2$ (COD = 1,5-cyclooctadiene) and $Re(CO)_5Cl$ gave *cis*-$Ru(tBuL\text{–}NS)_2(CO)_2$, Rh(*t*BuL–NS)(COD) and $Re(tBuL\text{–}NS)(CO)_4$, respectively. The structure of Rh(*t*BuL–NS)(COD) has been established by X-ray crystallography. The geometry around Rh is square planar with Rh–N and Rh–S distances of 2.114 (5) and 2.250 (2) Å, respectively. Reaction of $Ni(PMe_3)_2(CH_3)Cl$ with Li(*t*BuL–NS) afforded $Ni(tBuL\text{–}NS)(PMe_3)CH_3$, which undergoes CO insertion to give the acyl complex $Ni(tBuL\text{–}NS)(PMe_3)(COCH_3)$. The cyclic voltammogram of $Pt(tBuL\text{–}NS)_2$ exhibits a reversible 1-electron couple at 0.3 V *vs* ferrocenium–ferrocene, which is assigned as the ligand-centered oxidation. © 1997 Elsevier Science Ltd

Keywords: synthesis; electrochemistry; pyridine–thiolate complexes.

Metal–sulfur complexes have attracted much attention because of their resemblance to the active centers of metalloenzymes [1] and their potential application to homogeneous catalysis [2]. Recently Holm and coworkers have synthesized oxomolybdenum complexes of a bulky bidentate pyridine-thiolate ligand *t*BuL–NS (bis(4-*t*-butylphenyl)-2-pyridylmethanethiolate(1−)) as models for oxomolybdenum enzymes. Oxo transfer from *cis*-$MoO_2(tBuL\text{–}NS)_2$ to phosphines was observed and the structures of both *cis*-$MoO_2(tBuL\text{–}NS)_2$ and $MoO(tBuL\text{–}NS)_2$ have been established by X-ray crystallography. The salient feature of *t*BuL–NS is the steric bulk imposed by the *t*-butylphenyl group that precludes the biologically irrelevant μ-oxo-Mo^V dimer formation [3]. However the chemistry of metal complexes of the types $M(tBuL\text{–}NS)_2$ and $M(tBuL\text{–}NS)X_n$ (X = monodentate ligand) have not been explored. Herein we report the syntheses and electrochemistry of such complexes and the crystal structure of Rh(*t*BuL–NS)(COD).

RESULTS AND DISCUSSION

Syntheses of the $M(tBuL\text{–}NS)_2$ *and* $M_2(tBuL\text{–}NS)_2Cl_2$ *complexes*

The reactions of Li(*t*BuL–NS) with $NiCl_2$, $ZnCl_2$ and $PtCl_2(COD)$ afforded the respective bis-chelate complexes $M(tBuL\text{–}NS)_2$ (M = Ni (**1**), Zn (**4**), Pt (**9**)) in good yields. These complexes are soluble in toluene and chlorinated solvents but insoluble in hexane and methanol. The ^1H NMR spectra of $M(tBuL\text{–}NS)_2$ show a single resonant signal for the *t*-Bu groups, indicative of the symmetric coordination mode of *t*BuL–NS in these complexes.

Treatment of Li(*t*BuL–NS) with $CuCl_2$ gave the 1 : 1 dimeric complex $[Cu(tBuL\text{–}NS)Cl]_2 \cdot 2H_2O$ (**2**).

---

* Author to whom correspondence should be addressed.

Table 1. Crystallographic data for Rh(tBuL–NS)(COD) (**6**)

Formula	$C_{34}H_{42}NRhS$
M_r	599.7
Crystal system	monoclinic
Space group	$P2_1/n$
a (Å)	11.533 (2)
b (Å)	12.586 (2)
c (Å)	20.442 (2)
β (°)	96.06 (2)
U (Å^3)	2950.7 (8)
Z	4
ρ_{calc}/g cm^{-3}	1.35
Crystal size/mm	0.4 × 0.1 × 0.1
Color; habit	yellow needles
T/K	298
μ (min^{-1})	5.494
2θ range (°)	3.0–110.0
F(000)	1256
Independent reflections	3590 (R_{int} = 2.66%)
Observed reflections	2608 ($F > 4.0\sigma(F)$)
Weighting scheme	$w^{-1} = \sigma^2(F) + 0.0002F^2$
$R_F{}^a$	0.0430
$R_{WF}{}^a$	0.0436
GOF^b	1.38

${}^a R_F = \Sigma(|F_o| - |F_c|)/\Sigma(|F_o|)$; $R_{WF} = [\Sigma w(|F_o| - |F_c|)^2/\Sigma w |F_o|^2]^{1/2}$.

^{b}GOF $= [\Sigma w(|F_c| - |F_o|)^2/(N_{obs} - N_{param})]^{1/2}$.

The mass spectrum of **2** shows the molecular ion corresponding to the dimeric structure. Reaction of $Cu(OTf)_2$ (OTf = triflate) with Li(tBuL–NS) yielded a green crystalline solid analyzed as Cu_2(tBuL–NS)$_3$(OTf) (**3**). The formulation of **3** as a Cu^{II}–Cu^{II} dimer is tentative because the mass spectrum does not shows the molecular ion. The coordination modes of tBuL–NS in **2** and **3** are not clear. Complexes **2** and **3** are paramagnetic with μ_{eff} 1.6 and 1.7 μ_B, respectively, suggestive of antiferromagnetic coupling between the Cu centers in these complexes. Treatment of $PdCl_2(PhCN)_2$ with Li(tBuL–NS) afforded a red solid, analyzed [Pd(tBuL–NS)Cl] (**7**). This Pd^{II} complex is presumably dimeric and has a square planar geometry around each Pd as expected for d^8-configurated complexes.

Syntheses of cis-Ru(tBuL–NS)$_2$(CO)$_2$ *and* Re(tBuL–NS)(CO)$_4$

The ruthenium complex *cis*-[Ru(tBuL–NS)$_2$(CO)$_2$] (**5**) was prepared by the reaction of $[Ru(CO)_2Cl_2]_n$ with Li(tBuL–NS) in refluxing DMF. The IR spectrum of this complex displays two ν(C≡O) at 2035 and 1972 cm^{-1}, indicative of the *cis* disposition of the two carbonyl ligands. Consistent with this geometry, the ^{1}H NMR spectrum displays two singlets for the t-Bu groups. Complex **5** is very inert and does not react with pyridine and phosphines even under refluxing conditions.

Reaction of $Re(CO)_5Cl$ with Li(tBuL–NS) gave air-stable Re(tBuL–NS)(CO)$_4$ (**8**). The IR spectrum shows CO stretches at 2010 and 1908 cm^{-1}, which are slightly lower than those for the starting $Re(CO)_5Cl$. The mass spectrum displays the molecular ion corresponding to the [Re(tBuL–NS)(CO)$_3$] fragment.

Synthesis and crystal structure of Rh(tBuL–NS)(COD)

Reaction of $[Rh(CO)_2Cl]_2$ with Li(tBuL–NS) in THF gave an orange solution, from which a purple solid was isolated. The IR spectrum of this purple solid exhibits intense CO bands around 2000 cm^{-1}. The ^{1}H NMR spectrum of this purple solid shows more than one t-butyl resonant signals. The DCI mass spectrum displays the molecular ion corresponding to [Rh$_2$(tBuL–NS)$_2$(CO)$_4$]. However, we have not been able to obtain correct analytical data for this complex. Treatment of [Rh(COD)Cl]$_2$ with Li(tBuL–NS) gave Rh(tBuL–NS)(COD) (**6**), isolated as air-stable yellow crystals (see Table 1). The structure of the Rh complex has been characterized by X-ray crystallography. Figure 1 shows a perspective view of the molecule; selected bond lengths and angles are given in Table 2. As expected for 4-coordinate Rh^I complex, the geometry

Table 2. Selected bond lengths (Å) and angles (deg) for Rh(tBuL–NS)(COD) (**6**)

Rh(1)—S(1)	2.250 (2)	Rh(1)—N(2)	2.114 (5)
Rh(1)—C(1)	2.127 (8)	Rh(1)—C(4)	2.127 (8)
Rh(1)—C(5)	2.120 (7)	Rh(1)—C(8)	2.140 (6)
C(1)—C(8)	1.40 (1)	C(4)—C(5)	1.39 (1)
S(1)—Rh(1)—N(2)	83.5 (1)	S(1)—Rh(1)—C(1)	160.1 (2)
N(2)—Rh(1)—C(1)	98.7 (3)	S(1)—Rh(1)—C(4)	90.3 (2)
N(2)—Rh(1)—C(4)	163.9 (3)	C(1)—Rh(1)—C(4)	82.3 (3)
S(1)—Rh(1)—C(5)	92.1 (2)	N(2)—Rh(1)—C(5)	156.4 (3)
C(1)—Rh(1)—C(5)	93.3 (3)	C(4)—Rh(1)—C(5)	38.2 (3)
S(1)—Rh(1)—C(8)	161.6 (2)	N(2)—Rh(1)—C(8)	95.7 (2)
C(1)—Rh(1)—C(8)	38.2 (3)	C(4)—Rh(1)—C(8)	94.8 (3)
C(5)—Rh(1)—C(8)	81.3 (3)	Rh(1)—S(1)—C(10)	104.0 (2)

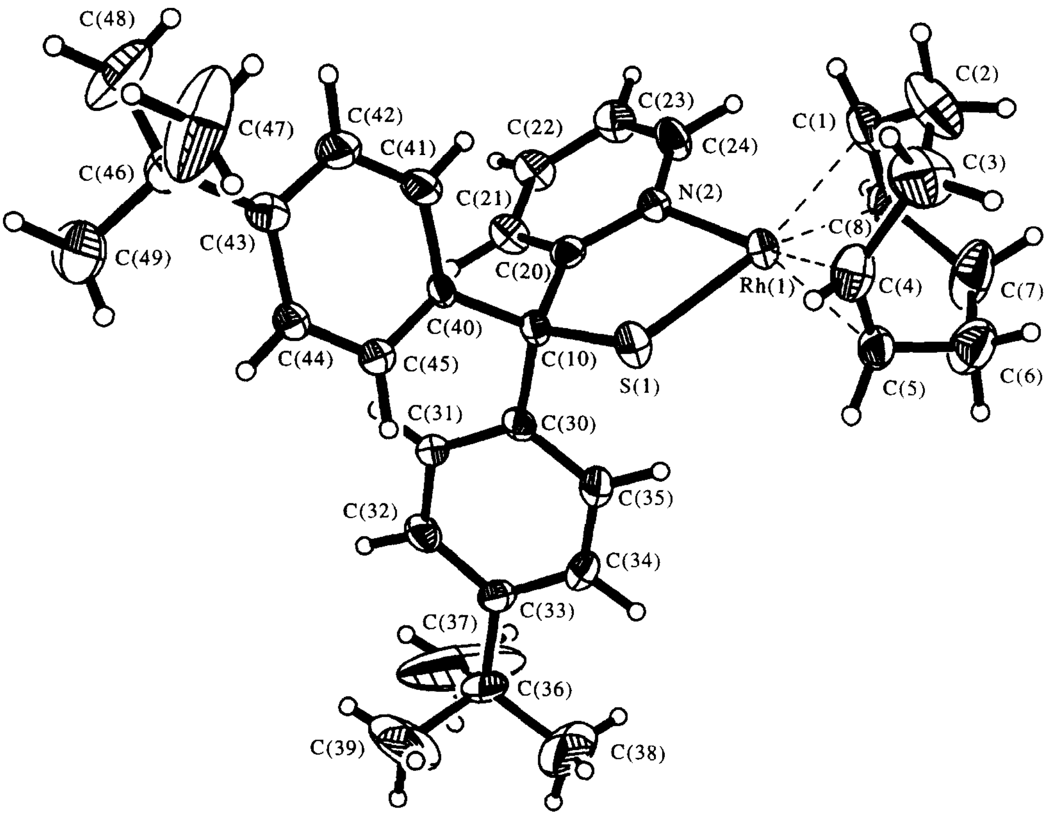

Fig. 1. Perspective view of Rh(*t*BuL–NS)(COD) (**6**).

around Rh is square planar. The Rh–C distances are comparable to those for $[Rh(COD)(\mu\text{-}SR)]_2$ (2.135 Å) [9]. The Rh–S distance of 2.250 (2) Å is shorter than that found in $Rh(SPh)(PMe_3)_3$ (2.428 (2) Å) [10]. The Rh—S—C angle of 104° is acute compared with other metal–thiolate complexes [11]. It should be noted that while dimeric thiolate-bridged Rh^I complexes are well documented, there are relatively few examples of terminal Rh^I thiolate complexes [13]. Apparently the steric bulk of 4-*t*-butylphenyl groups in *t*BuL–NS inhibits the formation of the thiolate-bridged dimer. The COD ligand in Rh(*t*BuL–NS)(COD) can be readily substituted by a variety of ligands such as phosphines and CO to give Rh(*t*BuL–NS)L_n (L = PR_3 or CO).

While Rh complexes containing carbonyl, phosphines and cyclopentadienyl are well-known catalysts for hydrogenation and the related organic transformations, there are relatively few studies on the Rh^I thiolate analogues [9,12,13]. Complex **6** was found to be a catalyst for hydrogenation of olefins under ambient conditions. For example, reaction of styrene with hydrogen under ambient conditions gave ethylbenzene in good yields, albeit rather slowly. The turnover number of 10 is rather low compared to the Rh^I–phosphine systems and possibly because of the slow COD dissociation from **6**, which is required to provide a vacant site for hydrogen activation.

Synthesis of Ni(*t*BuL–NS)(PMe_3)CH_3

Nickel alkyl complexes of thiolate ligands are of interest because such species are believed to be involved in the catalytic cycle of nickel-containing carbon monoxide dehydrogenase. Reaction of $Ni(PMe_3)_2(CH_3)Cl$ with Li(*t*BuL–NS) gave the Ni^{II} methyl complex Ni(*t*BuL–NS)$CH_3(PMe_3)$ (**10**), which was characterized by NMR spectroscopy. The ^1H NMR spectrum of **10** shows a singlet at δ −0.27 assignable to the methyl protons. Unfortunately we were not able to obtain good analytical data for **10** because the compound was found to be exceedingly air-sensitive. When a solution of **10** in C_6D_6 was bubbled with CO, the methyl resonance gradually decreased in intensity and a new singlet at δ 1.79 appeared. Evaporation of the solution gave a solid, which shows an intense IR band at 1629 cm^{-1}, characteristic of the —C═O stretch of an acyl group. This suggests the formation of the Ni^{II} acyl complex Ni(*t*BuL–NS)(PMe_3)[C(O)CH_3] via the insertion of CO to Ni—CH_3 bond (eq. 1).

$$Ni(tBuL\text{–}NS)(PMe_3)CH_3 + CO \rightarrow Ni(tBuL\text{–}NS)(PMe_3)[C(O)CH_3] \quad (1)$$

Therefore the singlet at δ 1.79 was assigned as the acyl methyl protons C(O)C*H*$_3$.

Table 3. Formal potentials (E^0) for the *t*BuL–NS Complexes[a]

Compound	E^0 (V *vs* $Cp_2Fe^{+/0}$) Oxidation	Reduction
Ni(*t*BuL–NS)$_2$	0.18 (70)	−1.92 (70)
Pt(*t*BuL–NS)$_2$	1.0[b], 0.30 (80)	
Ru(*t*BuL–NS)$_2$(CO)$_2$	0.42 (80)	−1.96[b]
Re(*t*BuL–NS)(CO)$_4$	0.30 (90)	

[a] Potentials measured in CH_2Cl_2 with 0.1 M $[Bu^n_4N]PF_6$ as supporting electrolyte; working electrode is glassy carbon, scan rate = 100 mV s^{-1}. ΔE_p values ($E_a - E_c$ in mV) are given in parentheses.

[b] Irreversible.

Electrochemistry

Table 3 summarizes the formal potentials (E^0) for the *t*BuL–NS complexes. The cyclic voltammogram (CV) of Ni(*t*BuL–NS)$_2$ (Fig. 2a) shows a reversible couple at *ca* −2.0 V (ΔE_p = 70 mV, $i_a/i_c \sim 1$) and an irreversible oxidation wave at +0.4 V *vs* $Cp_2Fe^{+/0}$. The reduction couple at −2.0 V is assigned to the metal-centered nickel(II)/(I) couple because no couple was found for Zn(*t*BuL–NS)$_2$ at this potential region. The nickel(II)/(I) couple for Ni(*t*BuL–NS)$_2$ was found at a more negative potential than those for the dithia dioxime analogue [Ni(Dtdo)]$^+$ (at −1.155 V *vs* Ag^+/Ag) [14] and the tetraaza macrocycle analogue Ni(tmtaa) (at −1.73 V *vs* $Cp_2Fe^{+/0}$) [15]. The irreversible wave at 0.4 V is possibly due to the oxidation of Ni^{II} to Ni^{III}. In contrast to other Ni^I complexes such as [Ni(cyclam)]$^+$ which reduce CO_2 electrocatalytically [16], the electrogenerated [Ni^I(*t*BuL–NS)$_2$]$^-$ species does not react with CO_2.

The electrochemistry of Pt–sulfur compounds is of interest because sulfur ligands are known to stabilize mononuclear Pt^{III} state [17,18]. The CV of Pt(*t*BuL–NS)$_2$ displays a reversible couple at *ca* 0.3 V (ΔE_p = 80 mV, $i_a/i_c \sim 1$) and an irreversible wave at 1.0 V. Controlled potential electrolysis at 0.6 V gives n = 1.01, indicating the former oxidation couple is a one-electron process. The optical spectrum of the oxidized species [Pt(*t*BuL–NS)$_2$]$^+$ shows an absorption maximum at *ca* 698 nm (ε_M = 793 M^{-1} cm^{-1}), giving rise to the pale green coloration (Fig. 3). The CV of [Pt(*t*BuL–NS)$_2$]$^+$ is virtually identical to that of the starting material, indicating that no decomposition took place during the electrolysis and the oxidation was chemically reversible. Indeed, treatment of Pt(*t*BuL–NS)$_2$ in CH_2Cl_2 with 1 equiv. of AgO_3SCF_3 gave a pale green solution, whose optical spectrum is identical to that obtained by the controlled-potential electrolysis. The EPR spectrum of the reaction mixture shows a broad signal with g value *ca* 2.002, which is characteristic for ligand-centered cation radical. Given the broad observed EPR signal and the absence of hyperfine coupling, the couple at 0.3 V is assigned as the ligand-centered [Pt(*t*BuL–NS)(*t*BuL–NS)]/[Pt(*t*BuL–NS)(*t*BuL–NS$^•$)]$^+$ couple. Attempts to isolate [Pt(*t*BuL–NS)(*t*BuL–NS$^•$)]$^+$ in pure form were not successful. Similarly the reversible couples at 0.42 and 0.3 V for Ru(*t*BuL–NS)$_2$(CO)$_2$ and Re(*t*BuL–NS)(CO)$_4$, respectively, are attributable to the ligand-centered oxidation.

EXPERIMENTAL

All solvents were purified by standard procedures and distilled prior to use. UV–vis spectra were obtained on a Milton Roy Spectronic 3000 diode-array spectrophotometer; infrared spectra (Nujol) on a Perkin–Elmer 16 PC FT-IR spectrophotometer and mass spectra on a Kratos MS80RFAQ spectrometer. ^1H NMR spectra, in $CDCl_3$ unless otherwise stated, were recorded on a JEOL EX400 spectrometer. Chemical shifts (δ, ppm) were reported reference to

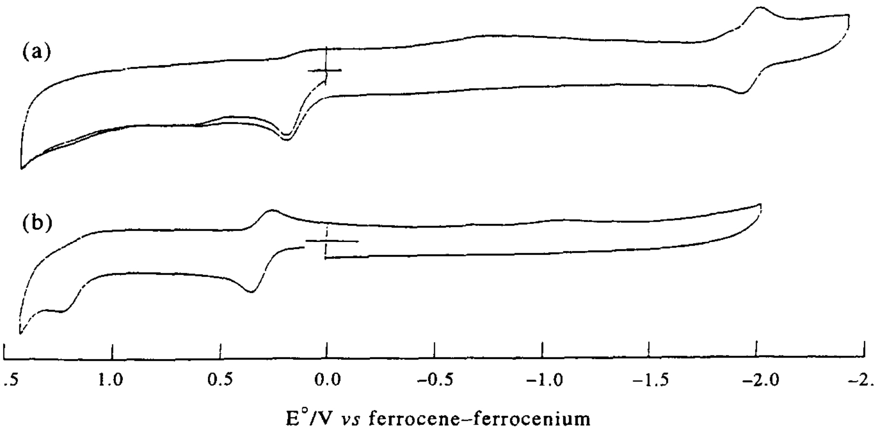

Fig. 2. Cyclic voltammograms for (a) Ni(*t*BuL–NS)$_2$ and (b) Pt(*t*BuL–NS)$_2$ in CH_2Cl_2 at a glassy carbon electrode. Scan rate = 100 mV s^{-1}.

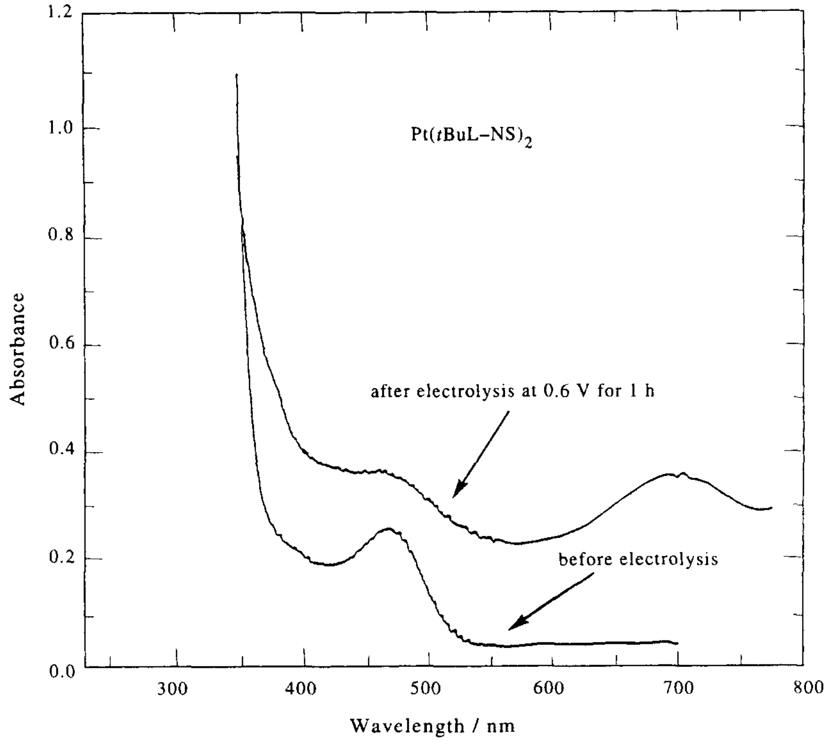

Fig. 3. Optical spectral change for the electrolysis of Pt(*t*BuL–NS)$_2$ at 0.6 V in 0.1 M $[Bu^n_4N]PF_6/CH_2Cl_2$.

$Si(CH_3)_4$. Hydrogen atom labeling scheme for *t*-BuL–NS complexes is shown in Scheme 1. Magnetic moments were measured by Evans method [4] at room temperature in $CHCl_3$ solutions. Cyclic voltammetry was performed with a Princeton Applied Research (PAR) Model 273A potentiostat. Potentials were controlled by with respect to Ag^+–Ag reference electrode in acetonitrile but are reported respect to the ferrocenium–ferrocene couple as measured in the same solution. Elemental analyses were performed by Medac Ltd., Brunel University, U.K.

The salt Li(*t*BuL–NS) [3b], $[Ru(CO)_2Cl_2]_n$ [5], $PdCl_2(PhCN)_2$ [6], $[Rh(COD)Cl]_2$ [7], $PtCl_2(COD)$ [8] (COD = 1,5-cyclooctadiene) and $Ni(PMe_3)_2(CH_3)Cl$ [9] were prepared by the literature methods. $Cu(OTf)_2$ (OTf = triflate) and $Re(CO)_5Cl$ were obtained from Strem Ltd. and used as received.

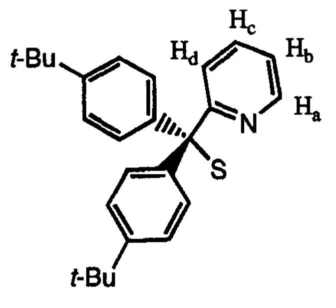

***t*BuL-NS**

Scheme 1.

Preparation of Ni(*t*BuL–NS)$_2$ (**1**)

To a solution of $NiCl_2$ (0.15 g, 0.63 mmol) in 20 cm^3 of CH_3OH was added Li(*t*BuL–NS) (0.16 g, 0.40 mmol) and the mixture was stirred at room temperature for 1 h. The yellow precipitate was collected, washed with CH_3OH, and recrystallized from CH_2Cl_2/hexane. Brown prisms formed were collected and washed with hexane (Yield 55%). ^1H NMR ($CDCl_3$) : δ 1.32 (s, 36H, *t*-Bu), 6.86 (t, 2H, H_c), 7.03 (d, 2H, H_d), 7.28 (d, 8H, H_m), 7.47 (d, 8H, H_0), 8.35 (t, 2H, H_c), 9.00 (d, 2H, H_a). UV–vis (CH_2Cl_2) : λ_{max} (nm)/ε (M^{-1} cm^{-1}) 288 (12,400), 350 (5450). MS (FAB) *m/z*: 836 (M^+). Anal. Calcd for $[C_{52}H_{60}N_2S_2Ni] \cdot CH_2Cl_2$: C, 69.1 ; H, 6.8 ; N, 3.0%. Found : C, 68.5 ; H, 6.9 ; N, 2.9%.

Preparation of $[Cu(tBuL\text{–}NS)Cl]_2 \cdot 2H_2O$ (**2**)

To a solution of $CuCl_2$ (0.15 g, 1.12 mmol) in 20 cm^3 of CH_3OH was added Lt(*t*(BuL–NS) (0.29 g, 0.73 mmol) and the mixture stirred at room temperature for 1 h. The solvent was removed in vacuo and the residue was extracted with CH_2Cl_2. Green crystals obtained by recrystallization from CH_2Cl_2/hexane were collected and washed with ether. (Yield : 35%). $\mu_{eff} = 1.6$ μB per Cu. UV–vis (CH_2Cl_2) : λ_{max}/nm (ε/M^{-1} cm^{-1}) 416 (1450), 722 (9120). MS (FAB) *m/z* : 974 (M^+). Anal. Calcd for $[C_{26}H_{30}NClSCu \cdot 2H_2O]$: C, 59.7 ; H, 6.5 ; N, 2.7%. Found : C, 60.1 ; H, 6.2 ; N, 2.6%.

Preparation of Cu$_2$(*t*BuL–NS)$_3$(OTf)·H$_2$O (**3**)

To a slurry of Cu(OTf)$_2$ (0.5 g, 1.38 mmol) in CH$_2$Cl$_2$ (25 cm^3) was added Li(*t*(BuL–NS) (1.09 g, 2.76 mmol) and the mixture was stirred at room temperature of night. The resulting green mixture was filtered, evaporated to dryness, and extracted with CH$_2$Cl$_2$. The filtrate was concentrated to 10 ml and layered with hexane. The dark green crystals were collected and washed with hexane (Yield 40%). μ_{eff} = 1.5 μB per Cu. IR (cm^{-1}): 1224, 1152, 1032 (triflate). Anal. Calcd for [C$_{79}$H$_{92}$N$_3$F$_3$O$_3$S$_4$Cu]: C, 65.0; H, 6.3; N, 2.9%. Found: C, 64.7; H, 6.3; N, 2.8%.

Preparation of Zn(*t*BuL–NS)$_2$ (**4**)

A mixture of ZnCl$_2$ (0.2 g, 1.47 mmol) and Li(*t*-BuL–NS) (0.58 g, 3 mmol) was stirred in CH$_3$OH (20 cm^3) at room temperature for 0.5 h, during which time a white solid was precipitated. The solid was collected, washed with CH$_3$OH, and recrystallized from CH$_2$Cl$_2$/hexane (Yield: 80%). ^{1}H NMR: δ1.35 (s, 36H, *t*-Bu), 6.82 (t, 2H, H$_c$), 6.94 (d, 2H, H$_d$), 7.05 (t, 2H, H$_b$), 7.21 (d, 8H, H$_m$), 7.29 (d, 8H, H$_o$), 7.55 (d, 2H, H$_a$). MS (DCI): *m/z* 840 (M—1)$^+$. Anal. Calcd for [C$_{52}$H$_{60}$N$_2$S$_2$Zn]: C, 74.2; H, 7.1; N, 3.3%. Found: C, 73.5; H, 7.3; N, 3.2%.

Preparation of cis-Ru(*t*BuL–NS)$_2$(CO)$_2$ (**5**)

A mixture of [Ru(CO)$_2$Cl$_2$]$_n$ (0.15 g, 0.66 mmol) and Li(*t*BuL–NS) (0.78 g, 1.98 mol) was heated under reflux in DMF (20 cm^3) under nitrogen overnight. The solvent was pumped off in vacuo and the residue extracted with CHCl$_3$. Evaporation of the CHCl$_3$ gave a yellow solid, which was recrystallization from CHCl$_3$/hexane (Yield 50%). ^{1}H NMR (CDCl$_3$): δ 1.25 (s, 18H, *t*-Bu), 1.33 (s, 18H, *t*-Bu′), 6.76, 7.10, 7.5 (m, 22H, aromatic), 10.03 (d, 2H, H$_a$). IR (cm^{-1}): 2035, 1972 ν(C≡O). UV-vis (CHCl$_3$): λ_{max}/nm (ε/M^{-1} cm^{-1}) 373 (1515). MS (FAB) *m/z* 934 (M), 878 (M—2 CO). Anal. Calcd for [C$_{52}$H$_{60}$N$_2$O$_2$S$_2$Ru]: C, 68.6; H, 6.6; N, 3.1%. Found: C, 67.9; H, 6.4; N, 2.9%.

Preparation of Rh(*t*BuL–NS)(COD) (**6**)

A mixture of [Rh(COD)Cl]$_2$ (0.1 g, 0.4 mmol) and Li(*t*BuL–NS) (0.16 g, 0.42 mmol) was stirred in 30 cm^3 of THF at room temperature overnight. The solvent was pumped off and the residue extracted with toluene. The toluene extract was evaporated to dryness to give a yellow solid which was recrystallized from toluene/hexane (Yield: 50%). ^{1}H NMR (CDCl$_3$): δ 1.30 (s, 18H, *t*-Bu), 1.88 (m, 4H, COD), 2.33 (m, 4H, COD), 3.97 (d, 2H, COD), 4.47 (d, 2H, COD), 7.10 (t, 1H, H$_c$), 7.17 (d, 4H, H$_m$), 7.24 (t, 1H, H$_c$), 7.35 (d, 1H, H$_d$), 7.56 (d, 1H, H$_b$), 7.86 (d, 4H, H$_o$). MS (FAB) *m/z*: 599 (M$^+$). UV–vis (CH$_2$Cl$_2$): λ_{max}/nm (ε/M^{-1} cm^{-1}) 283 (8280), 308 (7050), 420 (1210). Anal. Calcd for [C$_{34}$H$_{42}$NSRh]: C, 68.1; H, 7.0; N, 2.3%. Found: C, 68.7; H, 7.3; N, 2.1%.

Preparation of [Pd(*t*BuL–NS)Cl]$_2$ (**7**)

To PdCl$_2$(PhCN)$_2$ (0.5 g, 1.3 mmol) in THF (20 cm^3) was added Li(*t*Bu–LNS) (0.51 g, 1.3 mmol) and the mixture was stirred at room temperature for 2 h. The solvent was pumped off and the residue was extracted with CH$_2$Cl$_2$. The extract was evaporated to dryness leaving an orange solid, which was recrystallized from CH$_2$Cl$_2$/hexane to give orange crystals (Yield: 50%). ^{1}H NMR (CDCl$_3$): δ 1.28 (s, 18H, *t*-Bu), 1.32 (s, 18H, *t*-Bu), 6.88–7.62 (m, 22H, aromatic protons), 9.43 (d, 2H, H$_a$). UV–vis (CH$_2$Cl$_2$): λ_{max}/nm (ε/M^{-1} cm^{-1}) 275 (31,500), 305 (24,900). Anal. Calcd. for [C$_{52}$H$_{60}$N$_2$Cl$_2$S$_2$Pd$_2$]: C, 58.9; H, 5.8; N, 2.6%. Found: C, 60.5; H, 5.8; N, 3.0%.

Preparation of Re(*t*BuL–NS)(CO)$_4$ (**8**)

To a solution of Re(CO)$_5$Cl (100 mg, 0.28 mmol) in THF (25 cm^3) was added 1 equiv. of Li(*t*BuL–NS) (110 mg, 0.28 mmol) and the resulting orange mixture was stirred at room temperature overnight. The solvent was pumped off and the residue was extracted with CH$_2$Cl$_2$ and purified by column chromatography (neutral alumina). The product was eluted with CH$_2$Cl$_2$ and isolated as a pale yellow solid (Yield: 71%). ^{1}H NMR (CDCl$_3$): δ 1.19 (s, 9H, *t*-Bu), 1.27 (s, 9H, *t*-Bu′), 7.17 (t, 1H H$_c$), 7.29 (d, 4H, H$_m$), 7.42 (t, 1H, H$_b$), 7.61 (d, 4H, H$_o$), 7.98 (d, 1H, H$_d$), 9.18 (d, 1H, H$_a$). IR (cm^{-1}): 2010, 1908 ν(C≡O). MS(DCI): m/z: 658 (M—CO). UV-vis (CH$_2$Cl$_2$): λ_{max}/nm (ε/M^{-1} cm^{-1}) 266 (11,200), 310 (4230). Anal. Calcd for [C$_{30}$H$_{30}$NO$_4$SRe·H$_2$O]: C, 51.2; H, 4.5; N, 2.0%. Found: C, 51.6; H, 4.9; N, 2.1%.

Preparation of Pt(*t*BuL–NS)$_2$ (**9**)

A mixture of Pt(COD)Cl$_2$ (50 mg, 0.13 mmol) and 2 equiv. of Li(*t*BuL–NS) (0.11 g, 0.28 mmol) in THF (10 ml) was stirred at room temperature overnight. The precipitate was collected and recrystallized from CH$_2$Cl$_2$/hexane to give an orange microcrystalline solid (Yield: 75%). ^{1}H NMR: δ 1.30 (s, 36H, *t*-Bu), 6.96 (*t*, 2H, H$_c$), 7.04 (d, 2H, H$_d$), 7.24 (d, 8H, H$_m$), 7.40 (d, 8H, H$_o$), 7.64 (t, 2H, H$_b$), 9.50 (d, 2H, H$_a$). MS (FAB): *m/z* 971 (M$^+$). UV–vis (CH$_2$Cl$_2$): λ_{max}/nm (ε/M^{-1} cm^{-1}) 470 (603). Anal. Calcd for [C$_{52}$H$_{60}$N$_2$S$_2$Pt]: C, 64.2; H, 6.2; N, 2.9%. Found: C, 64.1; H, 6.2; N, 2.8%.

Reaction of **6** *with* CO

To a solution of **6** (5 mg) in C_6D_6 (0.7 cm^3) was bubbled with CO for 1 min. The resulting mixture was characterized to be [Rh(*t*BuL–NS)$(CO)_2$] by NMR and IR spectroscopy. ^{1}H NMR: δ 1.30 (s, 18H, t-Bu), 7.21–7.26, 7.73 (m, aromatic protons), 8.75 (d, 2H, H_a). Signals for free COD (δ 2.37 and 5.58) were also observed. IR (cm^{-1}): 2058, 1990 ν(C≡O).

Catalytic hydrogenation of styrene with **6**

A mixture of **6** (60 mg, 0.1 mmol) and styrene (0.115 cm^3, 1 mmol) was stirred in THF (10 cm^3) under hydrogen (1 atm) at room temperature for 2 days. An aloquot of sample was subject to GLC analysis. The yield of ethylbenzene was determined by GLC to be 95% with respect to styrene used.

Preparation of Ni(*t*BuL–NS)(PMe_3)CH_3 **(10)**

A mixture of Ni(PMe_3)(CH_3)Cl (100 mg, 0.38 mmol) and 1.2 equiv. of Li(*t*BuL–NS) (180 mg, 0.46 mmol) in THF (20 cm^3) was stirred at room temperature overnight. The solution was filtered and evaporated to dryness. The residue was extracted with ether and cooled at −40°C to give air-sensitive orange crystals (Yield: 70%). ^{1}H NMR ($CDCl_3$): δ −0.27 (d, 3H, CH_3), 0.93 (d, 9H, $P(CH_3)_3$), 1.22 (s, 18H, *t*-Bu), 6.30 (t, 1H, H_c), 6.61 (t, 1H, H_b), 6.78 (d, 1H, H_d), 7.21 (d, 4H, H_m), 7.58 (d, H, H_o), 8.46 (d, 1H, H_a).

Reaction of Ni(*t*BuL–NS)(PMe_3)CH_3 *with* CO

A solution of **10** (5 mg) in C_6D_6 (0.5 ml) was bubbled with CO for 30 s and the ^{1}H NMR spectrum of the resulting mixture was recorded. ^{1}H NMR (C_6D_6): δ 0.72 (d, 9H, $P(CH_3)_3$), 1.79 (s, 3H, $COCH_3$), 1.14 (s, 18H, *t*-Bu), 7.19 (d, 4H, H_m), 7.52 (d, 4H, H_o), 6.13, 6.51, 6.90 (m, 3H, pyridyl protons). 7.74 (d, 1H, H_a). Evaporation of the C_6D_6 solution gave a brown solid. IR (cm^{-1}): 1692 ν(C=O).

X-ray structure determination of Rh(*t*BuL–NS)(COD) **(6)**

A summary of the crystal and data processing data is given in Table 1 and selected bond lengths and angles are given in Table 2. Crystals of **6** were grown from a saturated CH_2Cl_2/ether solution of −10°C. Data were collected on a Siemens P4 diffractometer with graphite-monochromated CuKα radiation (λ = 1.54178 Å) at 298 K. Intensity data were corrected for Lorentz, polarization, and absorption effects. The structure was solved by Direct Methods and refined by full-matrix least-squares. All hydrogen atoms are refined isotropically and the hydrogen atoms were included in the idealized positions (C—H, 0.95 Å). Lists of final atomic coordinates, displacement factors and structure factors have been deposited as supplementary data with the Editor.

Acknowledgements—The financial support from the Hong Kong University of Science and Technology and the Hong Kong Research Grants Council is gratefully acknowledged.

REFERENCES

1. (a) Stiefel, E. I. and George, G. N., In *Bioinorganic Chemistry*, I. Bertini, H. B. Gray, S. J. Lippard and J. S. Valentine, Eds., University Science Books: Mill Valley, CA (1994), p. 365; (b) *Iron–Sulfur Proteins*, T. G. Spiro, Ed, Wiley-Interscience: New York (1985); (c) Armstrong, F., In *Adv. Inorg. Bioinorg. Mech.*, A. G. Sykes, Ed., Academic Press: New York, 1982, **1,** 1; (d) Holm, R. H., *Coord. Chem. Rev.*, 1990, **100,** 183; (e) Kim, J. and Rees, D. C., *Nature*, 1992, **257,** 1677; (f) Chan, M. K., Kim, J. and Rees, D. C., *Science*, 1993, **260,** 792.
2. Rakowski DuBois, M., *Chem. Rev.*, 1989, **89,** 1 and refs cited therein.
3. (a) Gheller, S. F., Schultz, B. E., Scott, M. J. and Holm, R. H., *J. Am. Chem. Soc.*, 1992, **114,** 6934. (b) Schultz, B. E., Gheller, S. F., Muetterties, M. C., Scott, M. J. and Holm, R. H., *J. Am. Chem. Soc.*, 1993, **115,** 2714. (c) Schultz, B. E. and Holm, R. H., *Inorg. Chem.*, 1993, **32,** 4244.
4. Evans, D., *J. Chem. Soc.*, 1959, 2003.
5. Colton, F. A. and Farthing, R. H., *Aust. J. Chem.*, 1971, **24,** 903.
6. Anderson, G. K., Lin, M., Sen, A. and Gretz, E., *Inorg. Synth.*, 1990, **28,** 60.
7. Giodano, G., Crabtree, R. H., Heintz, R. M., Foster, D. and Morris, D. E., *Inorg. Synth.*, 1990, **28,** 88.
8. Drew, D., Doyle, J. R. and Shaver, A. G., *Inorg. Synth.*, 1990, **28,** 346.
9. Hein, H.-F. and Harsch, H. H., *Chem. Ber.*, 1973, **106,** 1433.
10. Polo, A., Claver, C., Castillón, S., Ruiz, A., Bayón, J. C., Mealli, C. and Masi, D., *Organometallics*, 1992, **11,** 3525.
11. Osakada, K., Hataya, K. and Yamamoto, T., *Inorg. Chem.*, 1993, **32,** 2360.
12. Dilworth, J. R. and Hu, J., *Adv. Inorg. Chem.*, 1990, **40,** 411.
13. Dilworth, J. R., Miller, J. R., Wheatley, N., Baker, M. J. and Sunley, J. G., *J. Chem. Soc., Chem. Commun.*, 1995, 1579.
14. Claver, C., Castillón, S., Ruiz, N., Delogu, G., Fabbri, D. and Gladiali, S., *J. Chem. Soc., Chem. Commun.*, 1993, 1833.
15. Pavlishchuk, V. V., Addison, A. W., Butcher, R. J. and Kanters, R. P. F., *Inorg. Chem.*, 1994, **33,** 397.
16. Bailey, C. L., Bereman, R. D. and Rillema, D. P., *Inorg. Chem.*, 1986, **25,** 3149.
17. (a) Blake, A. J., Gould, R. O., Holder, A. J., Hyde, T. I., Lavery, A. J., Odulate, M. O. and

Schröder, M., *J. Chem. Soc., Chem. Commun.*, 1987, 118; (b) Bond, A. M., Colton, R., Fiedler, D. A., Kevekordes, J. E., Tedesco, V. and Mann, T. F., *Inorg. Chem.*, 1994, **33**, 5761.

18. (a) Fisher, B. and Eisenberg, R. J., *J. Am. Chem. Soc.*, 1989, **102**, 7361; (b) Beley, M., Collin, J.-P., Ruppert, R. and Sauvage, J.-P., *J. Chem. Soc., Chem. Commun.*, 1984, 1315.